# CHAPTER 5

## Synthesis and E-metrics studies of an $SO_4^{-2}/CoAl_2O_4$-$TiO_2$ heterogeneous acid catalyst for production of solketal

## 5.1 Introduction

This chapter deals with the synthesis of a new heterogeneous catalyst by coprecipitation and wetness impregnation process and its application in solketal synthesis. No reports have been found on the efficient synthesis of $SO_4^{-2}/CoAl_2O_4$-$TiO_2$ solid acid catalyst and its catalytic application in glycerol acetalization. The selection of design concepts suggests that the new solid acid composite, $SO_4^{-2}/CoAl_2O_4$-$TiO_2$, is likely to exhibit improved acid properties and enhanced structural stability. Hence, the current study shows the synthesis of $SO_4^{-2}/CoAl_2O_4$-$TiO_2$ catalyst that is applied for solketal synthesis and got excellent glycerol conversion at optimized reaction conditions. The designed catalyst is acidic, non-toxic, and environment-friendly in nature. The influence of various mass ratio of $CoAl_2O_4/TiO_2$ and their catalytic efficiency towards the synthesis of solketal from bio-waste glycerol assisted with acetone was characterized through several characterization tools, including FTIR, TGA, BET, XRD, SEM-EDX, acid-base titration, and XPS. The green metrics studies of the modified catalyst showed that the synthesis route, from glycerol to solketal, was environmentally benign and eco-friendly in nature. Synthesized solketal was also characterized by $^1H$, $^{13}C$ NMR, and GCMS analysis.

## 5.2 Catalyst synthesis process

$SO_4^{-2}/CoAl_2O_4$-$TiO_2$, an acid heterogeneous catalyst, was prepared by co-precipitation, followed by the simple impregnation process. Initially, $CoAl_2O_4$ was synthesized via a co-precipitation process using metal nitrate precursor at a constant pH range. First of all, the required amount of cobalt nitrate and aluminum nitrate with a molar ratio of 1:2 was taken in a separate beaker and dissolved in distilled water. The solution was mixed in a single beaker and constantly stirred for 3-4 h at 35 $^oC$. Dropwise addition of ammonia to maintain the pH of the solution ~ 8-10. After precipitation, the reaction mixture was left under continuous stirring overnight. Then, the precipitate was filtered out from the mother

liquor and washed with distilled water to remove impurity ions. The precipitate was dried overnight at 90 $^{o}$C in an oven and then calcined at 700 $^{o}$C in a muffle furnace for 5 h to obtain the $CoAl_2O_4$. After that, a considered amount of $CoAl_2O_4$ and $TiO_2$ were mixed in a single beaker, dissolved with distilled water, stirred for 3 h at 40 $^{o}$C, and then evaporated the mixture at 80 $^{o}$C. The required powder was incorporated with 0.5 M $H_2SO_4$ solution to enhance the acidic properties of the designed catalyst by impregnation process for 4-5 h. Afterward, the final powders were dried in an oven at 110 $^{o}$C and then calcined at 500 $^{o}$C in an air muffle furnace for 3 h to get the desired $SO_4^{-2}/CoAl_2O_4$-$TiO_2$ catalysts. The different mass ratios of $CoAl_2O_4$ and $TiO_2$ were named as including $SO_4^{-2}/CoAl_2O_4$ (1:0) (SC), $SO_4^{-2}/CoAl_2O_4$-$TiO_2$ (3:2) (SCAT 3:2), $SO_4^{-2}/CoAl_2O_4$-$TiO_2$ (2:3) (SCAT 2:3), $SO_4^{-2}/CoAl_2O_4$-$TiO_2$ (4:1) (SCAT 4:1), $SO_4^{-2}/CoAl_2O_4$-$TiO_2$ (1:4) (SCAT 1:4) and $SO_4^{-2}/TiO_2$ (0:1) (ST), respectively. The obtained catalyst was stored in a desiccator for further application in solketal synthesis.

All the synthesized catalysts were applied for solketal synthesis, and their stability and catalytic activity were checked by performing various characterization techniques.

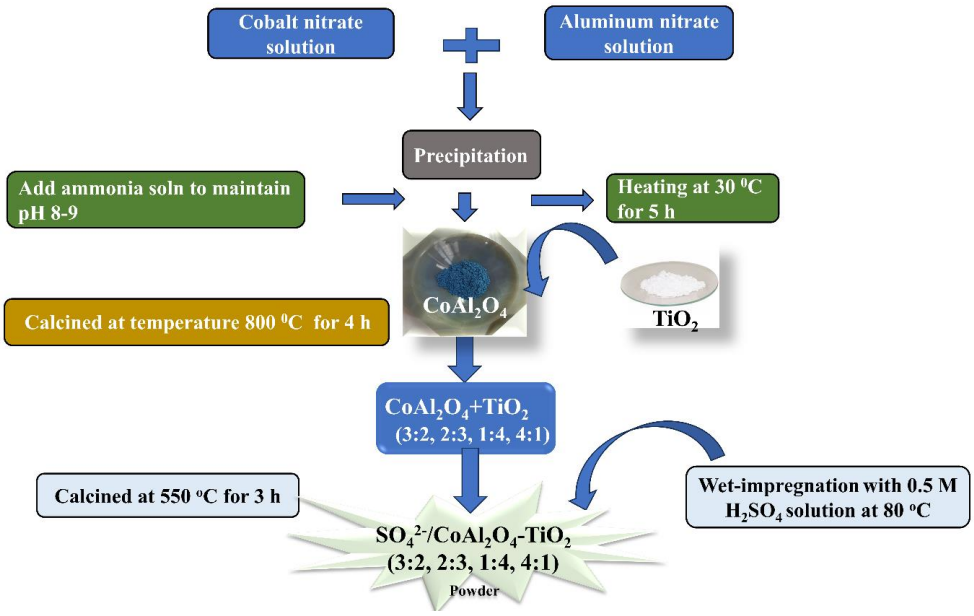


**Scheme 5.1 Synthesis of modified catalyst**

## 5.3 Characterization of synthesized catalyst

### 5.3.1. TGA analysis

To investigate the thermal stability of the synthesized SC, ST, and SCAT catalysts, the uncalcined catalyst was subjected to a TGA analysis to examine weight loss versus temperature. Figure 5.1 displays the TGA graph of the catalyst, which shows three regions of weight loss. The first weight loss occurred in the temperature range of 100 $^{o}$C to 220 $^{o}$C, attributed to removing the physically bound water molecule on the catalyst surface. The second weight loss of the sample was observed around 220 $^{o}$C to 550 $^{o}$C, which might be attributed to the desorption of the chemically bound water molecule from the catalytic surface. With a further increase of temperature even more than 550 $^{o}$C, the third weight loss started to be associated with the decomposition of the sulfate group on the catalyst surface. According to the TGA profile, the weight percentage of sulfate groups removed from the surface of SC, ST, and SCAT catalysts were estimated and observed to be 2.4%, 1.3%, and 6.0%, respectively. The decrease in weight loss indicates that both $TiO_2$ and $CoAl_2O_4$ acted as active components and showed a sulfate group on the catalyst surface [117,118]. Thus, it was concluded that SCAT (3:2) showed more weight loss, i.e., contained more sulfate group, which might be due to the presence of both $CoAl_2O_4$ and $TiO_2$ components.

The decomposition temperature of these synthesized catalysts indicates that SC shows better thermal stability than ST catalysts. This result revealed that $CoAl_2O_4$ acts as a structural stabilizer by enhancing the thermal stability of uncalcined synthesized SCAT (3:2) catalysts.

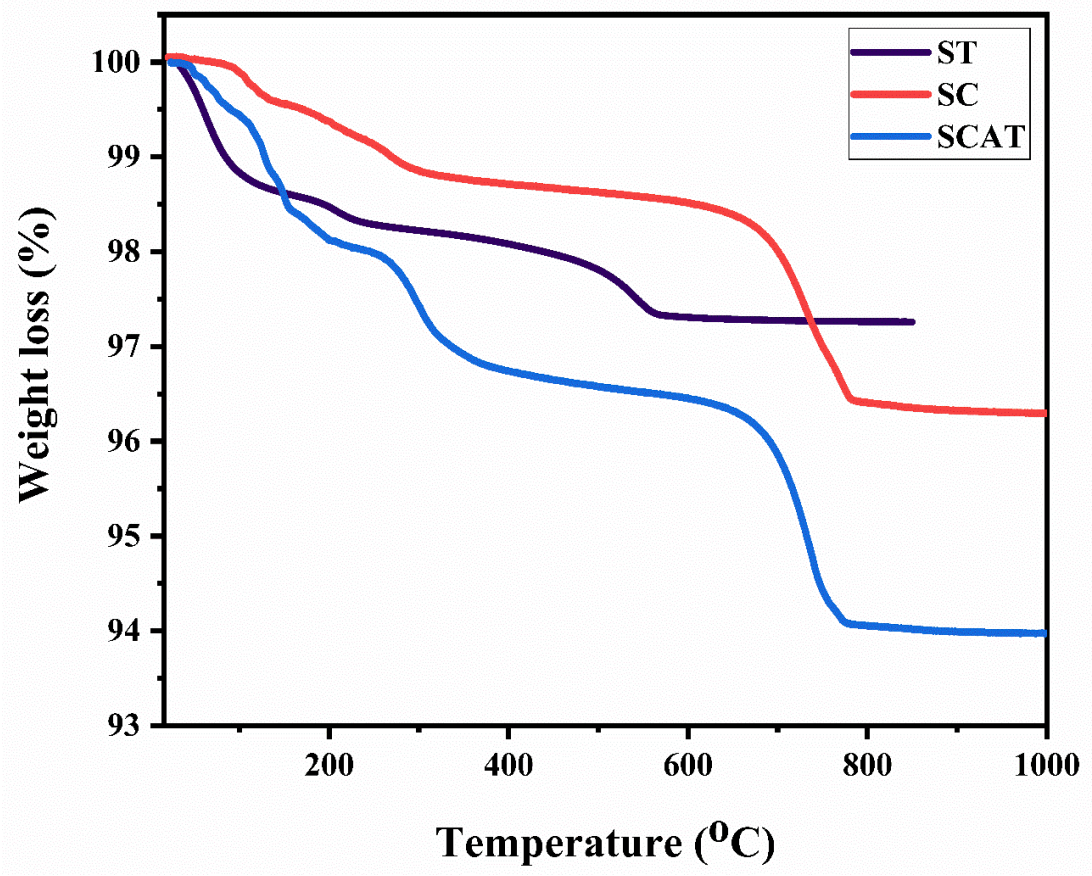


**Figure 5.1 TGA plot of uncalcined catalyst**

### 5.3.2. X-ray diffraction studies

Figure. 5.2 shows the X-ray diffractogram of $SO_4^{-2}/CoAl_2O_4$ (SC), $SO_4^{-2}/TiO_2$ (ST), and $SO_4^{-2}/CoAl_2O_4$-$TiO_2$ (SCAT) catalysts. The characteristics diffraction peaks obtained at 2θ equal to 20.8, 36.0, and 54.9 with corresponding miller indices (400), and (511) shows the formation of cubic $CoAl_2O_4$ (JCPDS file no. 3-0896) were present in the SC and SCAT catalysts. The other peaks at 2θ values 25.3, 37.5, 47.9, 53.7, and 62.6 with corresponding miller indices (101), (004), (200), (105), and (204), respectively, indicate the presence of the anatase phase of $TiO_2$ (JCPDS file no. 65-5714), observed in ST and SCAT catalyst. Another prominent diffraction peaks were observed at 15.1, 25.3, 30.5, 33.2, and 40.6, with the planes of miller indices (012), (113), (024), (116), and (303), respectively, indicating the formation of $Al_2(SO_4)_3$ (JCPDS no. 42-1410). Besides these,

other small reflection peaks at 27.3, 34.1, 38.5, 43.2, and 54.9 with the miller indices (201), (121), (221), (202), and (040), respectively, confirmed the existence of α-$CoSO_4$ (JCPDS no. 46-0004)[117,119]. All these diffraction peaks were observed in the SCAT catalyst, showing the sulfate group's successful impregnation. The intensity of diffracted peaks was changed by varying the molar concentration of these two components.

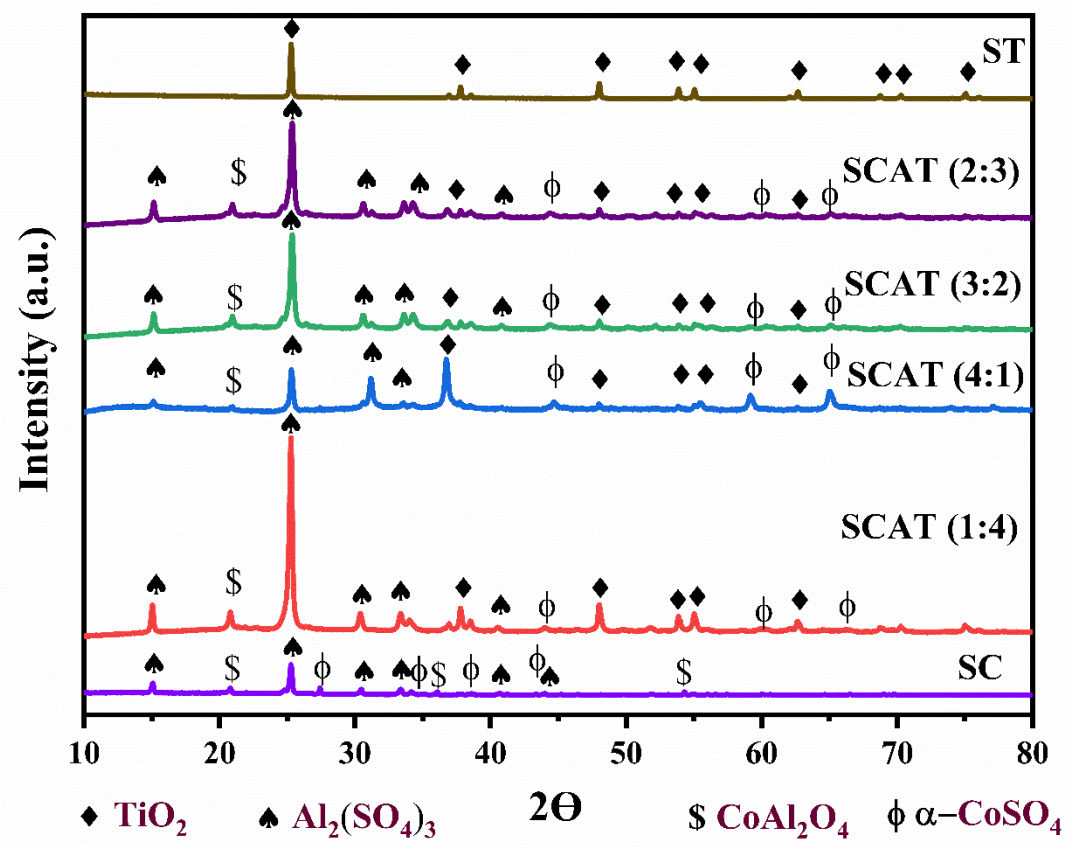


**Figure 5.2 XRD patterns of synthesized catalyst**

### 5.3.3. FTIR spectra

The presence of surface functional groups in synthesized SC, ST, and SCAT catalysts was studied through FTIR analysis and depicted in Figure 5.3. The broad peaks observed at 1329 and 1183 $cm^{-1}$ were assigned to the asymmetric and symmetric stretching vibrations of the S=O groups, while the other peaks appeared at 1086 and 921 $cm^{-1}$, indicating the existence of asymmetric and symmetric vibration of S− O bonds,

respectively [120]. In addition, the characteristics of the broad peak observed at 400-800 $cm^{-1}$ might be attributed to the stretching vibration of the Ti-O-Ti bond in ST. In contrast, this broad peak was not observed in SCAT spectra, possibly due to an intense band of Co-O and Al-O stretching vibration. The stretching vibration in the 545 $cm^{-1}$ to 683 $cm^{-1}$ range explains the Al-O bond, while the peaks observed below 500 $cm^{-1}$ are responsible for the Co-O vibration peak for $CoAl_2O_4$ spinel in all SCAT catalysts [119]. Another characteristic peak at 1651 $cm^{-1}$ is ascribed to the bending vibration of the O-H group of water molecules, whose intensity decreases with increasing the loading percentage of $TiO_2$. The broad peak at 3385 $cm^{-1}$ was due to the stretching vibration mode of physically bound water molecules on the catalytic surface.

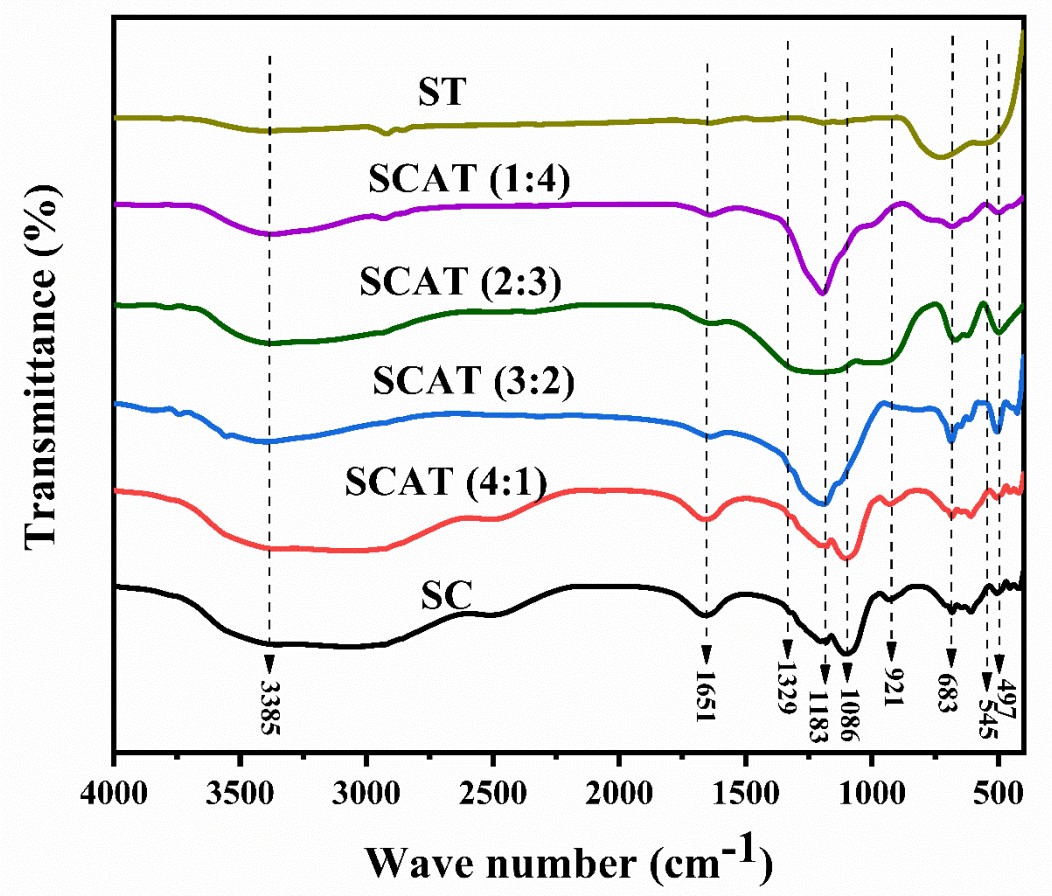


**Figure 5.3 FTIR spectra of catalyst**

### 5.3.4. SEM-EDX analysis

The morphology of the synthesized catalyst was analyzed by the Scanning Electron Microscope and depicted in Figure 5.4. Figure. 5.4 (a) portrays the image of pure SC illustrating the irregular-shaped particles with variable grain size on the catalyst's surface. Figure 5.4 (b) shows that the particles of ST are aggregated to form agglomerates and show an irregular spherical shape on the catalyst surface with different grain sizes. The FE-SEM image of SCAT (3:2) reveals the presence of both $CoAl_2O_4$ and $TiO_2$ on the composite surface and maintains their unique morphology, as depicted in Figure 5.4 (c) [121,122]. Moreover, the composite SCAT morphology reveals the incorporation of irregular $CoAl_2O_4$ particles on the surface of the $TiO_2$ bulk. The SEM image of the 5th cycle reused catalyst (RSCAT) showed a similar morphology to that of the fresh catalyst and confirmed the stability of the reused catalyst, as shown in Figure 5.4 (d). The existence of the elements on the catalyst's surface, like Co, Ti, Al, O, and S, was analyzed by the EDX (Energy dispersive X-ray) spectra. With the help of the EDX report, it was found that both the weight % and atomic % of Co are high in the synthesized catalyst, confirming the synthesis of 3:2 stoichiometry of Co and Ti in the SCAT (3:2) catalyst. The obtained EDX report is illustrated in Figure 5.4 (e).

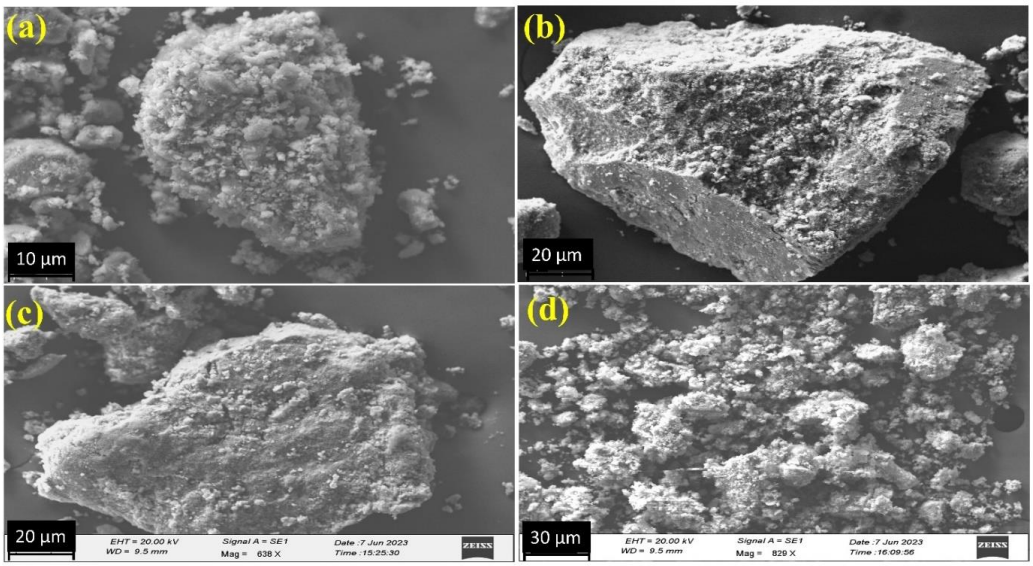

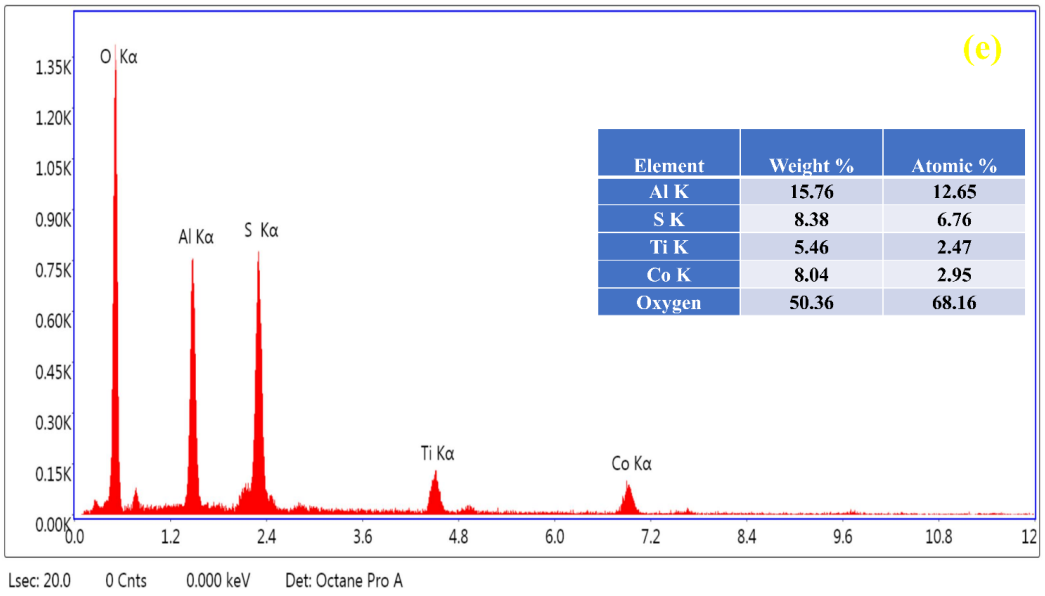


| Element | Weight % | Atomic % |
|---|---|---|
| Al K | 15.76 | 12.65 |
| S K | 8.38 | 6.76 |
| Ti K | 5.46 | 2.47 |
| Co K | 8.04 | 2.95 |
| Oxygen | 50.36 | 68.16 |

**Figure 5.4 FE-SEM image of (a) SC, (b) ST, (c) SCAT (3:2), (d) Reused SCAT catalyst at 550 ºC, and (e) EDX spectra of SCAT (3:2) catalyst**

### 5.3.5. BET surface area analysis

The surface properties of the synthesized SC, ST, and SCAT (3:2) catalysts were quantified through $N_2$- adsorption-desorption isotherm and shown in Figure 5.5. The specific surface area, pore volume, and pore diameter of the synthesized catalyst were determined by BET- BJH method and the obtained results are illustrated in Table 5.1. According to the IUPAC classification, the acquired isotherms exhibit hysteresis loop features indicative of Type-IV isotherms, which are linked with capillary condensation, thereby verifying the presence of mesostructured materials. The obtained result indicates that after the dispersion of $TiO_2$ over $CoAl_2O_4$ spinel, no changes were observed in the mesoporous nature of the modified catalyst. The specific surface area of SCAT (3:2), in which SC modified with ST, was 6.7 $m^2/g$; the decrease in the surface area could be attributed to the incorporation of ST in the lattice site of SC surface [123,124].

(a)

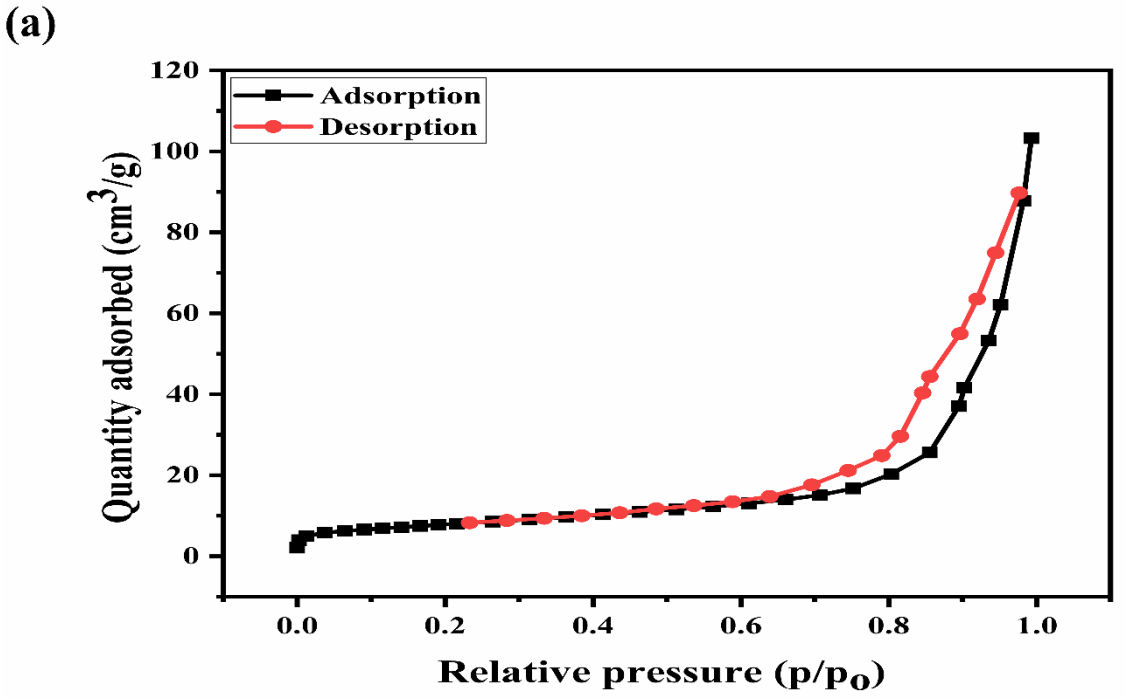
Adsorption
Desorption
Quantity adsorbed (cm3/g)
Relative pressure (p/po)
0
20
40
60
80
100
120
0.0
0.2
0.4
0.6
0.8
1.0

(b)

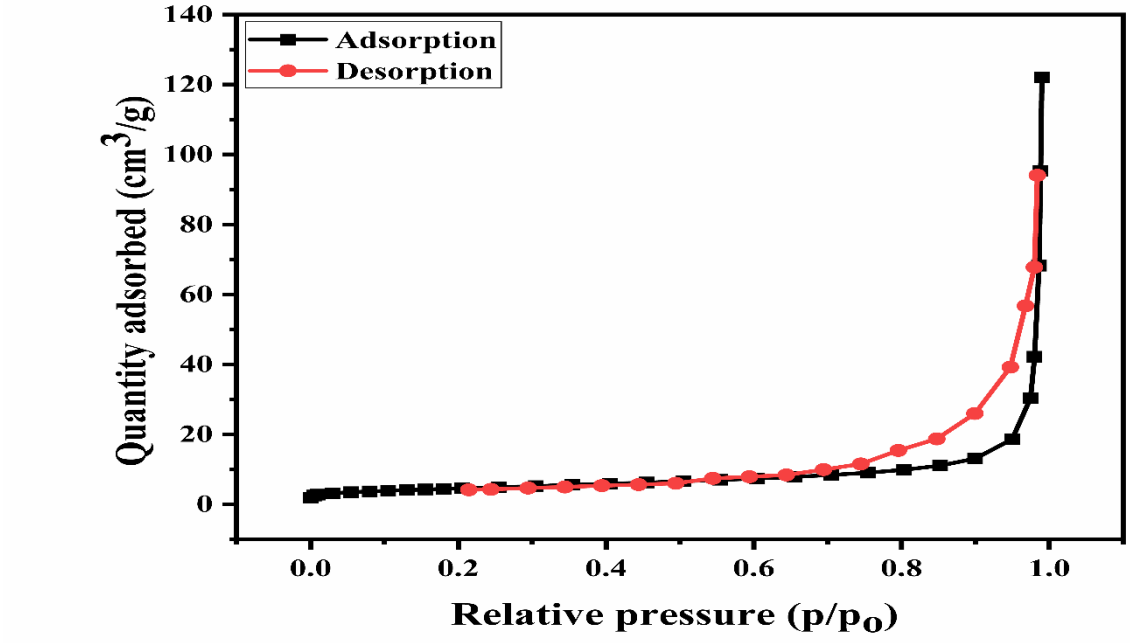
Adsorption
Desorption
Quantity adsorbed (cm3/g)
Relative pressure (p/po)
0
20
40
60
80
100
120
140
0.0
0.2
0.4
0.6
0.8
1.0

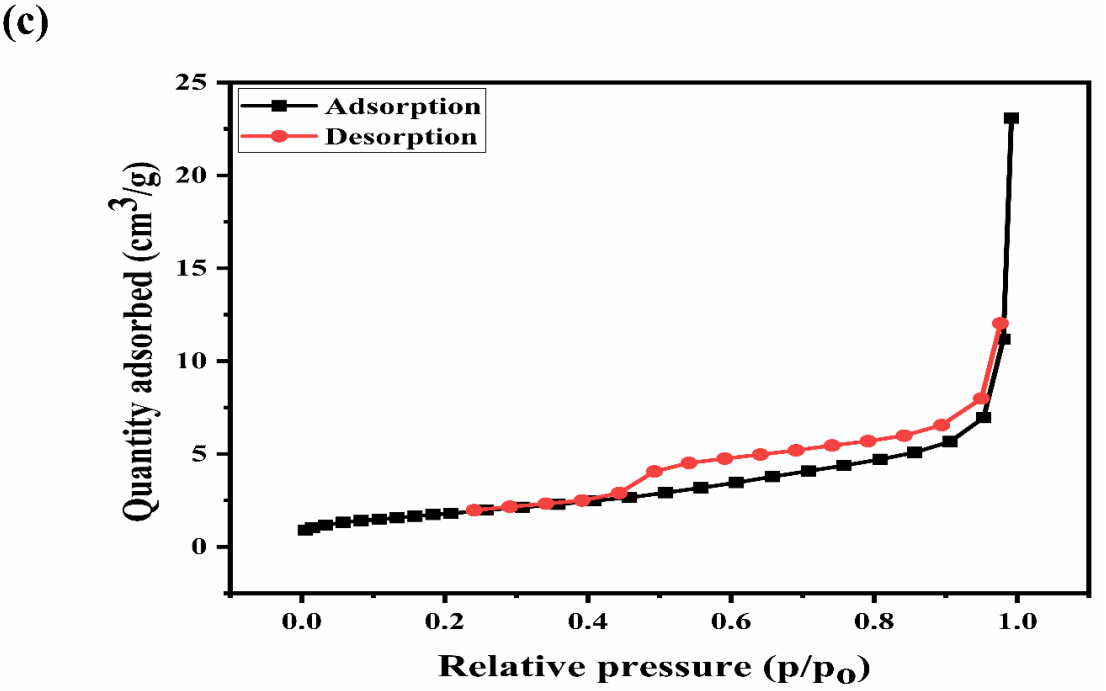


**Figure 5.5 Nitrogen adsorption-desorption isotherm of (a) SC, (b) ST, and (c) SCAT (3:2) catalyst.**

**Table 5.1. Surface properties of the designed catalyst**

| Catalysts | BET surface area ($m^2/g$)[a] | Specific pore volume ($cm^3/g$)[b] | Average pore diameter (nm)[c] |
|---|---|---|---|
| **SC** | 27.9 | 0.15 | 20.4 |
| **ST** | 16.2 | 0.17 | 38.4 |
| **SCAT(3:2)** | 6.7 | 0.03 | 17.0 |

[a] The BET-specific surface area was analyzed through BET method,

[b] Specific pore volume through the adsorbed amount of nitrogen ($p/p_0$=0.99), and

[c] BJH method used to calculate average pore diameter

### 5.3.6. XPS analysis

The catalyst's surface oxidation state and chemical composition were measured through XPS (X-ray photoelectron spectroscopy), and the obtained graphs are portrayed in Figure 5.6. The obtained spectra showed the existence of Co, Al, Ti, O, and S elements on the modified catalyst's surface. The Co 2p spectra possess two characteristics, binding energy peaks at 781.8 eV and 798.1 eV, which correspond to the Co $2p_{3/2}$ and Co $2p_{1/2}$,

respectively separated by a splitting value of 15.3 eV, might be due to the spin-orbit coupling of Co 2p assigned to the +2-oxidation state of Co. The other two peaks observed at 785.5 eV and 803.2 eV show the shake-up satellite peaks of Co $2p_{3/2}$ and Co $2p_{1/2,}$ respectively [125]. The main peak at 169.4 eV binding energy corresponds to the 2p spectra of sulfur, confirming the $S^{+6}$ oxidation state. The high oxidation state of sulfur evidences the existence of the bidentate sulfate group. This indicates that catalysts possessed acidic sites [126]**.** The 2p spectrum of Ti shows the two deconvoluted peaks appear at binding energies of 459.0 eV, which signifies Ti $2p_{3/2}$ and 464.7 eV assigned to the Ti $2p_{1/2,}$ respectively, revealing that titanium exists in a +4-oxidation state. Similarly, the characteristics peak of the 2p spectrum of Al observed at 75.3 eV corresponds to the +3-oxidation state ($Al^{+3}$). In addition, oxygen 1s spectra show three deconvoluted peaks at 531.4, 532.3, and 533.2 eV, respectively. The peak at 531.4 eV confirms the formation of lattice oxygen of metal oxide, and the other peak at 532.3 eV attributed to the bridged oxygen of the surface hydroxyl groups, and the peaks at 533.2 eV corresponds to the surface sulfate oxygen, respectively [127]. The obtained result agrees with the NIST and Thermo Fisher XPS databases.

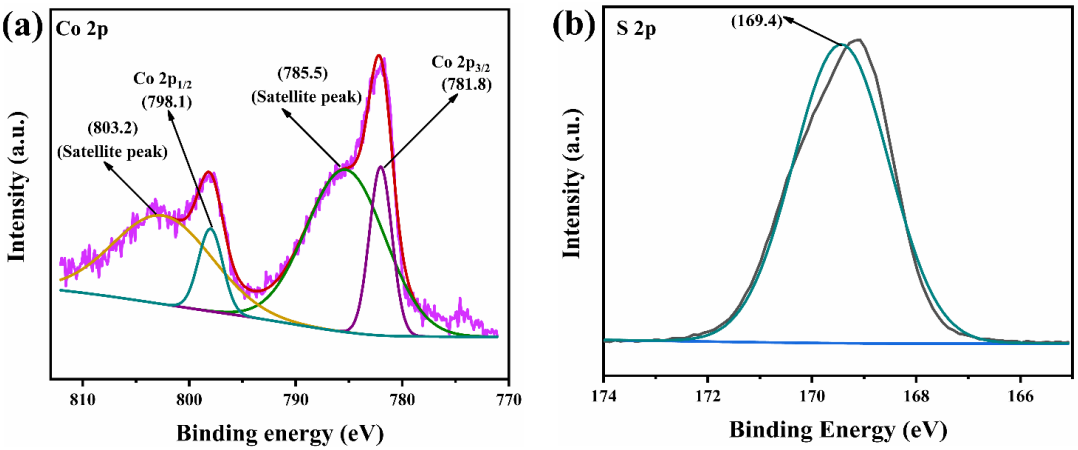

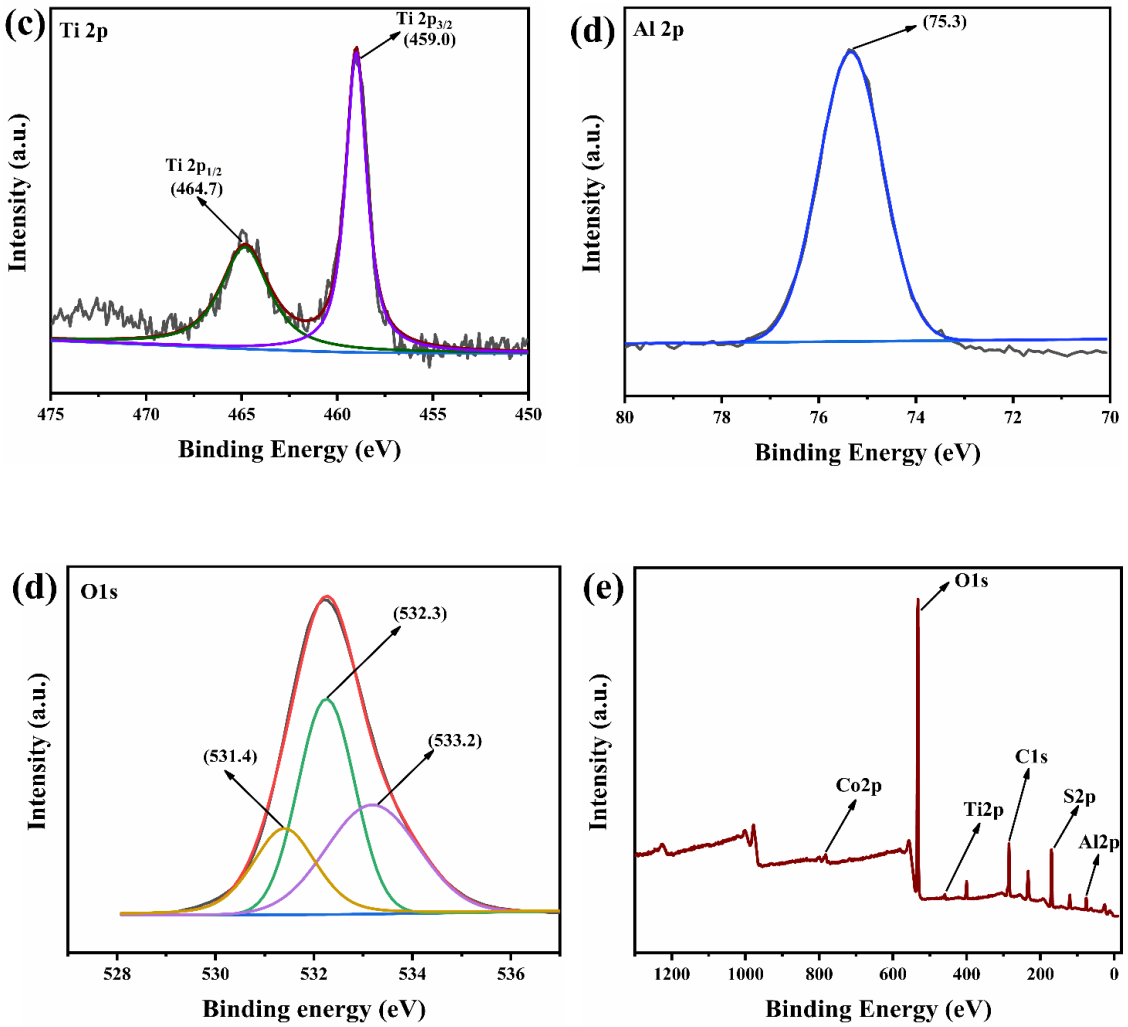


**Figure 5.6 XPS spectra of (a) Co 2p, (b) S 2p, (c) Ti 2p, (d) Al 2p, (e) O 1s, and (f) survey peak of synthesized SCAT (3:2) catalyst**

### 5.3.7. Acidity of the synthesized catalyst

The acidic strength is an important factor that plays a crucial role in the acetalization reaction of glycerol to solketal. Moreover, the calculation of acidic strength and acidity of the synthesized catalyst with different mass ratios is highly needed and examined by using an N-butylamine titration method. The different amounts of $CoAl_2O_4$ and $TiO_2$ strongly affected the acidic site of the catalyst. It was found that when the amount of $TiO_2$ increased, the acidic sites increased. However, the excess amount creates a negative impact and decreases the acidic strength on the catalyst surface. The decrease in acidic strength might be due to the accumulation of $TiO_2$ particles on the $CoAl_2O_4$ surface[127]. The $SO_4^{-2}/CoAl_2O_4$-$TiO_2$ (3:2) catalyst has more significant acidic sites than $SO_4^{-2}/TiO_2$

and $SO_4^{-2}$ /$CoAl_2O_4$, which are sufficient for better glycerol conversion illustrated in Table 5.2. During the reaction mechanism, the acidic site of the catalyst plays a crucial role in carbonyl carbon's protonation, facilitating the nucleophilic attacks of the -OH group on carbonyl carbon.

**Table 5.2 Screening of catalyst for solketal synthesis**

| Catalyst | Acidic sites (mmol/g)[a] | Conversion (%)[b] | Yield (%)[b] | TOF (mol $g^{-1}h^{-1}$)[c] | Crystallite size (nm)[d] |
|---|---|---|---|---|---|
| **SC** | 1.8 | 77 | 67 | 0.13 | 33 |
| **SCAT (1:4)** | 1.7 | 71 | 64 | 0.12 | 32 |
| **SCAT (2:3)** | 1.6 | 68 | 60 | 0.11 | 16 |
| **SCAT (3:2)** | 2.34 | 99 | 98 | 0.18 | 14 |
| **SCAT (4:1)** | 2.1 | 89 | 81 | 0.16 | 28 |
| **ST** | 1.9 | 82 | 73 | 0.14 | 45 |

[a] Acidic site was determined by N-butylamine titration,

[b] Conversion of glycerol and solketal yield by using Gas Chromatography-Mass Spectra and

[c] TOF (mol $g^{-1}h^{-1}$) by taking a number of moles of glycerol and per gram of catalyst per hr.

[d] Crystallite size was calculated using the Scherrer equation.

**5.4 Catalytic evaluation for solketal synthesis**

The catalytic efficiency of the designed catalyst was well executed by acetalization reaction in 100 ml of a two-neck round bottom flask attached to a reflux condenser. In order to provide equal heating and stirring to the reaction mixture, the reactor system was emersed in a silicone oil bath. During the reaction process, a thermometer was utilized to monitor the reaction temperature. The whole setup was situated on a magnetic stirrer. During the catalytic experiment, initially, 21.9 mmol of glycerol and 219 mmol of acetone were taken in a flask along with 0.10 g of a catalyst to the weight of glycerol and allowed to be stirred vigorously at 550 rpm at 58 $^oC$ temperature for 120 min. Once the reaction

reached completion, the flask was left to cool down to room temperature. Subsequently, the resulting liquid product was separated from the solid reaction mixture using simple filtration techniques employing Whatman filter paper. The catalyst, after being reused, underwent washing with chloroform and methanol for 3-4 cycles to facilitate its subsequent reuse in the glycerol acetalization reaction [128,129]. Then the obtained liquid product underwent quantitative analysis by using GC-MS analysis carried out using an Agilent Technologies, Inc. 7890B gas chromatograph coupled with a 19091P-MS4 mass spectrometer with capillary column HP-5 (30m ×0.32mm×0.25 micro m) and 1,4 – dioxane used as an internal standard. Besides GC-MS, $^{1}$H, and $^{13}$C-NMR spectroscopy were also performed to verify the obtained desired product. The modified catalyst's turnover frequency (TOF) was analyzed and represented in Table 5.2. The estimated TOF value demonstrates the efficient catalytic activity of the synthesized catalyst toward solketal production.

### 5.4.1. Characterization of synthesized product

#### 5.4.1.1. $^{1}$H and $^{13}$C NMR analysis

The synthesized product was examined by NMR spectroscopy to confirm the product formation by examining the obtained chemical shift value with the corresponding characteristics peak. Figure 5.7 (a) shows the $^{1}$H NMR spectroscopy of synthesized solketal, which was found to have various peaks at different chemical shift values. The two characteristic peaks observed at 1.26 and 1.30 ppm, which refers to the six- hydrogen of methyl, and the broad singlet peak observed at chemical shift value 2.0 ppm show the existence of a – OH group present in the cyclic ring. The multiplet peak observed at 3.37-4.80 ppm shows the total integration of -CH and -$CH_2$ groups that confirm the solketal synthesis from glycerol. Figure 5.7 (b) shows the $^{13}$C NMR of synthesized solketal. The NMR peak was found at 25.89 and 27.15 ppm, showing the methyl carbons of solketal. The characteristics peak of the cyclic ring (-$CH_2$-CH-$CH_2$-) emerged at 76.86 ppm, while

other peaks observed at 66.62 and 63.53 ppm are responsible for the two -$CH_2$ group of cyclic solketal. The deshielded ketal carbon peak was obtained at 108.71 ppm, and the conversion of glycerol to cyclic solketal was confirmed. The peak that appeared around 39.89 ppm corresponds to the DMSO-$d^6$ solvent. These two spectra indicate that a five-membered cyclic solketal is selectively formed over a six-membered ring during the acetalization of glycerol [130].

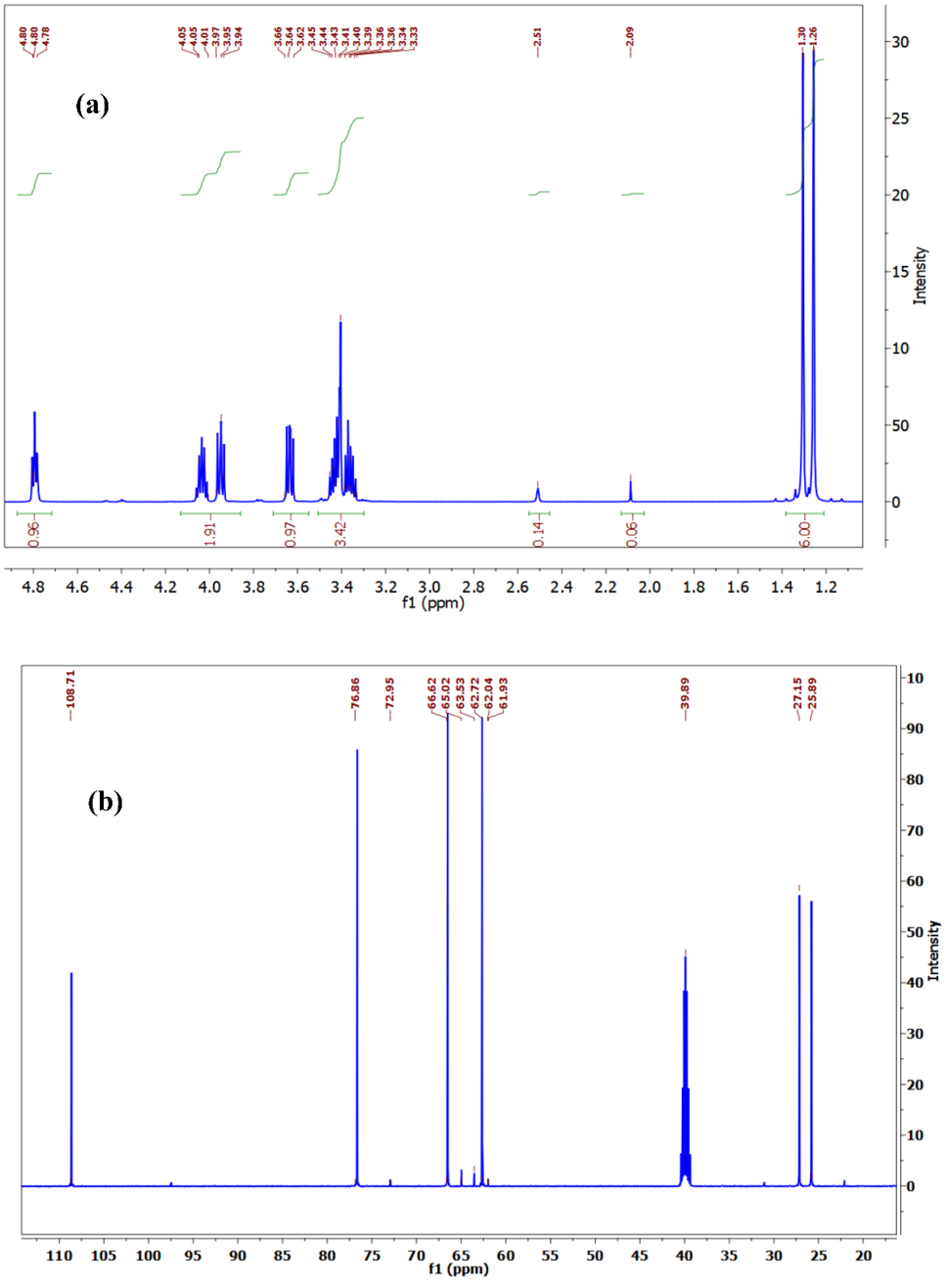


**Figure 5.7 (a) 1H NMR spectra, (b) 13C NMR spectra of solketal at optimized reaction conditions**

### 5.4.1.2. GC-MS studies of synthesized solketal

To calculate the quantitative analysis of the synthesized product, GC-MS (gas chromatography-mass spectroscopy) was performed, and the obtained peak is illustrated in Figure 5.8. The retention peak at 3.9 min confirmed the formation of a five-membered ring solketal, whereas the peak at 4.2 min for a six-membered acetal. The retention peak was observed at 4.8 min. denotes the quantity of glycerol that is not converted into the product[59]. The selectivity of the synthesized product is illustrated in Table 5.3.

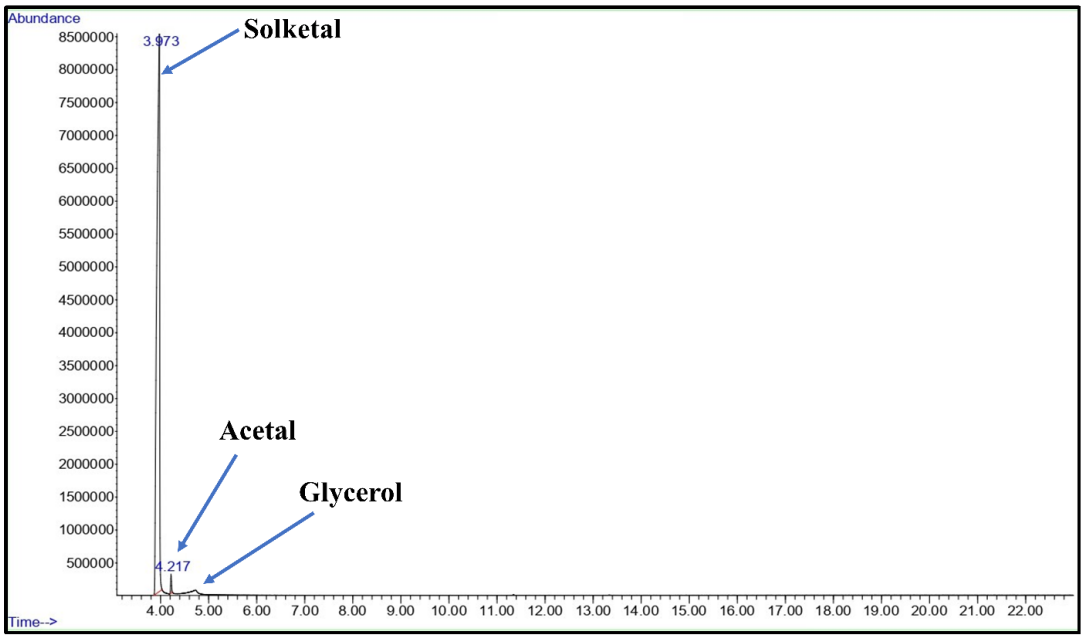


**Figure 5.8 GC-MS spectra of synthesized solketal**

**Table 5.3. Selectivity and Yield of the five and six-membered product using a catalyst**

| Catalyst | Conversion (%) | Selectivity (%) | | Yield (%) | |
|---|---|---|---|---|---|
| | | Solketal | Acetal | Solketal | Acetal |
| **SC** | 77 | 88 | 12 | 67.7 | 9.2 |
| **SCAT (1:4)** | 71 | 90 | 10 | 63.9 | 7.1 |
| **SCAT (2:3)** | 68 | 89 | 11 | 60.5 | 7.4 |

| | | | | | |
|---|---|---|---|---|---|
| **SCAT (3:2)** | 99 | 99 | 1 | 98 | 0.9 |
| **SCAT (4:1)** | 89 | 92 | 81 | 81.8 | 72 |
| **ST** | 82 | 90 | 10 | 73.8 | 8.2 |

### 5.5 Proposed reaction pathway for solketal synthesis

A plausible reaction pathway for solketal synthesis was proposed on the basis of the previously reported literature. This involves the condensation of acetone with glycerol in the influence of a SCAT catalyst, as shown in Figure 5.9. In this mechanism, metals act as a support for sulfonated catalysts, provide structural stability, and influence the acidity and surface properties of the synthesized catalyst by forming the chelating complex**.** Metals also stabilize the intermediate ion, by stabilizing their charge and facilitating the subsequent steps in the further reaction mechanism. This reaction mechanism follows the Langmuir-Hinshelwood (LH) type mechanism and proceeds in many steps**.** Firstly, the reactant molecule (glycerol and acetone) diffuses on the catalyst's surface and adsorbs on the pore of the catalyst. 1$^{st}$ step involves the acetone carbonyl group strongly coordinated with the Bronsted acid sites of the SCAT catalyst's strong acidic site to create the carbenium ion, which has a very short lifetime and is unable to be extracted. Afterward, 2$^{nd}$ step involves the formed carbenium ion undergoing nucleophilic attacks accompanied by the -OH of glycerol on electrophilic carbonyl carbon. Furthermore, 3$^{rd}$ step involves deprotonation, which produces hemiacetal intermediate. This intermediate is short lives highly unstable species and undergoes cyclization at a very fast rate to form a five-membered ring known as solketal and a six-membered cyclic ring acetal. When the secondary -OH group participates in the cyclization, a five-membered ring is produced, and a six-membered ring is also produced by the participation of the primary -OH group with the elimination of water. This mechanism supports solketal synthesis with 99 %

selectivity over six-membered acetal [59].

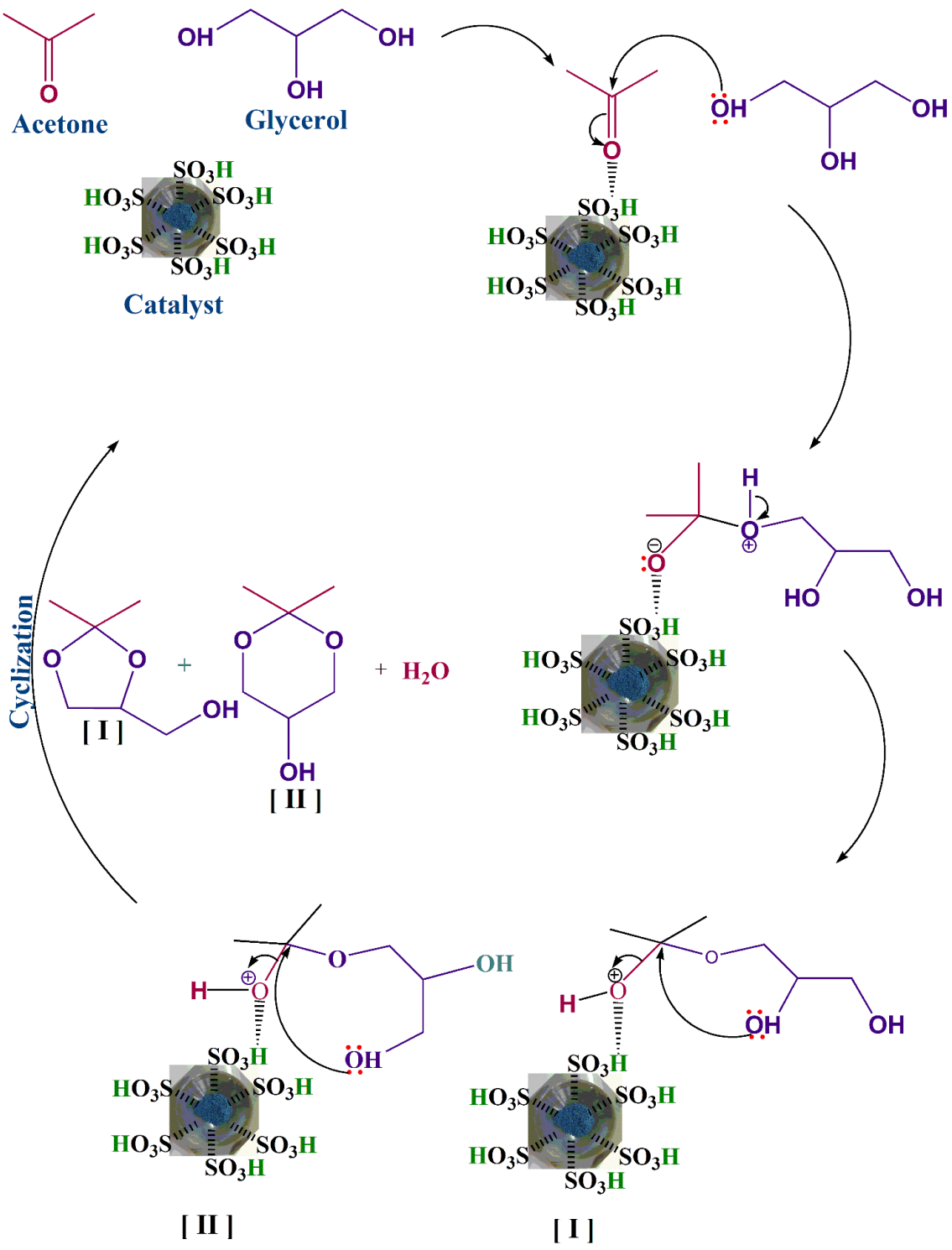


**Figure 5.9 A plausible reaction mechanism for solketal synthesis using SCAT catalyst**

## 5.6 Studies of optimization reaction parameters on solketal yield

### 5.6.1. Study of reaction temperature

The reaction temperature, one of the important parameters in the glycerol acetalization reaction, was studied by varying the reaction temperature from 28 $^{o}$C to 78 $^{o}$C while keeping the other reaction-affecting parameters to be constant (i.e., gly: ace molar ratio = 1:10, time = 120 min, catalyst loading = 3 wt.%). The influence of reaction temperature on glycerol conversion and solketal yield is shown in Figure 5.10 (a). At 28 $^{o}$C, the glycerol conversion was very low, i.e., 35 % was observed. Further increasing the reaction temperature from 38 to 58 $^{o}$C, the glycerol conversion percentage subsequently increases from 52 % to 99 %. This indicates that on increasing the reaction temperature, conversion and yield of reaction increase, which could be attributed to the number of collisions between glycerol and acetone molecule increases. Furthermore, a suitable reaction temperature helps in glycerol conversion by improving the miscibility of glycerol in acetone and also improves the reaction kinetics. Further, with a rise in the reaction temperature i.e., above 58 $^{o}$C, yield percentage, and glycerol conversion decrease drastically. The decline in conversion might be due to the evaporation of acetone (b. p. 56 $^{o}$C). As a result, glycerol conversion decreases due to the insufficiency of acetone molecules in the reaction matrix. Since the acetalization reaction of glycerol is exothermic, shifting towards a backward direction, decreases the glycerol conversion. However, the SCAT catalyst allows the reaction to reach the equilibrium faster at that temperature. Hence, it was observed that 58 $^{o}$C is the optimum temperature for solketal production[131]. Glycerol acetalization reaction was also performed at 2 atm under the same reaction conditions but did not get a significant result.

### 5.6.2. Influence of reaction time

Reaction time is another parameter that affects the glycerol acetalization reaction. The

influence of reaction time on solketal yield was studied and shown in Figure 5.10 (b) while keeping other reaction parameters as same (i.e., T = 58 $^{o}$C, gly: ace molar ratio = 1:10, catalyst loading = 3 wt.%). It was observed that with an increase in reaction time from 30 min to 120 min, the conversion of glycerol increases from 45 % to 99 % and solketal yield substantially increases from 43 % to 98 % respectively, which might be ascribed to the number of accessible reacting molecules increasing; as a result, new bonds are formed after breaking of the pre-existing bond. However, above 120 min, both solketal yield and glycerol conversion were decreased. A decrease in conversion was found, which could be due to the hydrolysis of the product facilitated by the formation of water during the reaction process [132]. Upon reaching equilibrium, the excess byproduct water can trigger the reaction in a backward direction by interacting with the solketal product, leading to the reverse reaction where solketal breaks down back into reactants.

### 5.6.3. Effect of glycerol to acetone molar ratio

The influence of glycerol to acetone molar ratio on the conversion of glycerol and solketal yield was explored by varying the molar ratio from 1:2 to 1:20 while keeping other reaction parameters constant, as shown in Figure 5.10 (c). As the molar ratio of glycerol and acetone increases from 1:2 to 1:10, the glycerol conversion percentage rises from 53% to 99% with 99 % selectivity towards five-membered solketal. Initially, acetone is poorly miscible in glycerol. As a result, low glycerol conversion was observed at low acetone concentrations while further increasing the acetone concentration in the reaction matrix; the synthesized solketal yield increases, which acts as a solubilizing agent and helps in better glycerol conversion. The increase in glycerol conversion was observed due to the availability of an excess amount of acetone, shifting the equilibrium toward the product side, which helps in product formation. A lower amount of acetone increases the viscosity of the reaction matrix, decreasing the glycerol conversion by reducing the

homogenization of glycerol and acetone. Further increase of glycerol and acetone molar ratio from 1:10 to 1:20, a minute decline in glycerol conversion was observed. This might be due to the saturation of the available active site of acetone that reacts with glycerol [133].

### 5.6.4. Study of catalyst weight percentage

The catalyst amount is another parameter affecting the glycerol conversion and product yield. Observations indicated that augmenting the catalyst weight percentage while maintaining other variables was the same (i.e., T = 58 $^{o}$C, gly: ace molar ratio = 1:10, time = 120 min) enhances glycerol conversion, and the results are illustrated in Figure 5.10 (d). In the absence of a catalyst, no glycerol conversion was observed. The glycerol conversion gradually increased from 40 to 99 % on increasing the catalyst from 0.5 wt.% to 3 wt.%. The increment in glycerol and solketal yield conversion could be ascribed to the number of available acidic active sites on the catalyst surface increases that promote the interaction and collision between the reacting molecules. Below 0.5 wt. % catalyst, a significant solketal yield cannot be observed due to the unavailability of enough acidic active sites. However, above 3 wt.% of catalyst amounts, solketal yield decreases due to the hydrolysis of the product. These findings align with those reported in a previous study. As a result, it was observed that 3 wt.% is the optimum catalyst amount for the high solketal yield [134].

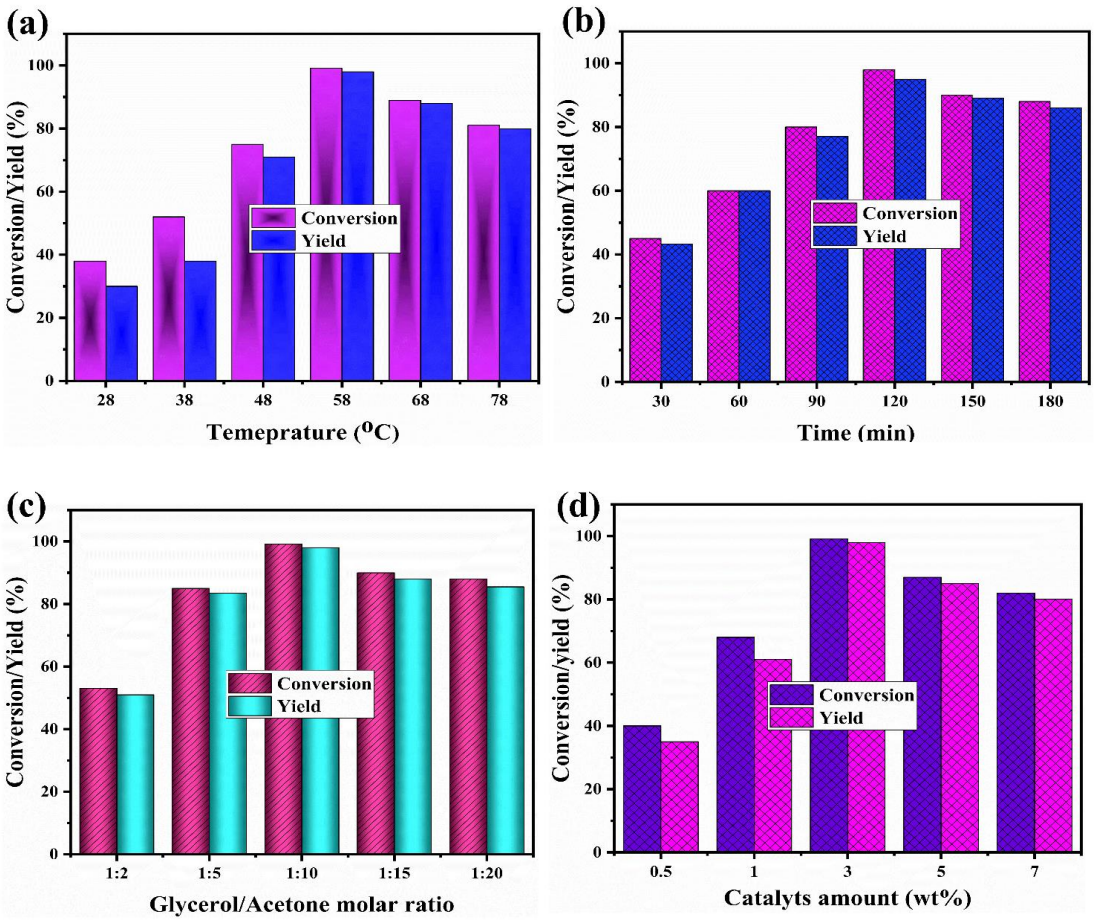


**Figure 5.10 Effect of reaction parameters on acetalization catalyzed by SCAT (3:2) catalyst (a) reaction temperature, (b) reaction time, (c) glycerol/acetone molar ratio, and (d) catalyst amount**

### 5.7. Green metrics studies in glycerol acetalization

According to the green chemistry postulates, the reaction process producing less waste is considered greener or cleaner. This means a cleaner pathway of any chemical reaction produces less waste. Thus, it becomes more important to investigate how much waste is generated during the catalytic reaction process. To know the effect of modified SCAT catalysts in the solketal synthesis on the environment was studied via various types of green metrics studies such as environmental factor (E- factor), process mass intensity (PMI), and carbon efficiency (CE). These studies give information about the eco-friendly route of the heterogenous acid-catalyzed acetalization of glycerol. The green metrics

calculation has been calculated under the same reaction condition as the acetalization reaction was performed. The optimized reaction conditions for green metric calculation were a 1:10 molar ratio of glycerol to acetone for 120 minutes of reaction duration at 58 $^{o}$C with 3 wt.% of catalyst loading.

The E- factor is the ratio of the waste mass produced during the acetalization to the desired product.

$$\text{E-factor} = \frac{Total\ mass\ of\ the\ waste\ (mg)}{Mass\ of\ the\ desired\ product\ (mg)} \quad (5.1)$$

A lower value of the E-factor indicates that less waste is generated during solketal synthesis and causes a positive impact on the environment. Water is formed as a by-product during the synthesis of solketal and can be utilized in other chemical reactions, so it is not regarded as a waste. The unreacted acetone was recovered by using rotatory evaporation for further glycerol acetalization reaction. The calculated value of the E-factor for glycerol acetalization was 0.084, indicating that the acetalization process is a green pathway for solketal synthesis. An ideal value of E- factor lies in the range of 0-1. Process mass intensity is another green parameter that deals with the sustainability of synthetic routes. This may consider the ratio of the total amount of all the materials applied in the reaction process, like catalysts, reactants, solvents, and reagents, to the isolated product. Mathematically, it can be expressed as

$$\text{Process Mass Intensity} = \frac{Total\ mass\ of\ all\ the\ materials\ used\ in\ solketal\ synthesis\ (mg)}{Mass\ of\ isolated\ product\ (mg)} \quad (5.2)$$

In this case, the acetalization is a solvent-free mechanism, and its value depends on the amount of catalyst, acetone, and glycerol used and the total mass of the solketal. The calculated value of PMI for this process was 1.87. Similarly, carbon efficiency (CE) is another green metric that was also studied in glycerol acetalization and found to be the

eco-friendly nature of the process. These green metrics studies may be defined as

$$CE\% = \frac{No.of\ moles\ of\ solketal \times no.of\ carbon\ in\ solketal \times 100}{Moles\ of\ glycerol \times no.of\ carbon\ in\ glycerol + no.of\ moles\ of\ acetone \times no.of\ carbon\ in\ acetone} \quad (5.3)$$

The obtained value of CE for solketal was estimated to be 0.66, which falls between 0-1. Since the carbon efficiency achieved by applying the SCAT catalyst lies in this range, it demonstrates that the synthesis process follows the greener route. This concluded that solketal synthesis follows an environmentally eco-friendly pathway, and the entire acetalization procedure is environmentally benign in nature [135].

**5.8 Reusability study of the catalyst**

Reusability study plays an important role in examining the catalyst's activity and stability. The loss of activity of the catalyst indicates the loss of acidity, which is responsible for the decrease in glycerol conversion. Here, we evaluated the acidity of the catalyst after each catalytic cycle using the N-butylamine titration method and obtained results tabulated in Table 5.4. After each successive batch, the consumed catalyst was separated by a simple filtration process and rinsed with chloroform and methanol 3-4 times to remove the adsorbed impurities from the catalyst surface. Afterward, the recovered catalyst was kept in an oven at 70 $^{o}$C for further solketal synthesis, as shown in Figure 5.11. The SCAT catalyst was reusable up to the 6$^{th}$ catalytic cycle with appreciable glycerol conversion; after 1$^{st}$ catalytic cycle, the glycerol conversion was decreased and found to be 95 % in 2$^{nd}$ run, and afterward, a slight decrease in glycerol conversion was observed and showed 84 % glycerol conversion in the 6$^{th}$ catalytic cycle. The decrease in conversion could be due to the loss of acidity from the catalyst surface. The authors compared it with another catalyst, as mentioned in Table 4, and found that the SCAT catalyst shows slight changes in glycerol conversion after 1$^{st}$ catalytic cycle than others. In addition, the synthesized sulfonated catalyst gives a maximum solketal yield of 98 %,

indicating SCAT catalyst's better performance compared to other mentioned sulphonic acid-based solid catalysts. After the 6$^{th}$ catalytic cycle, glycerol conversion was decreased to 75%, possibly due to the significant loss in the catalyst's active site. A leaching test was performed using Sheldon's hot-filtration method to determine the reason behind the decrease in glycerol conversion. During the process, 0.10 gm of catalyst dissolved with 37 ml of acetone was taken in a round bottom flask and heated at 58 $^{o}$C for two h at constant stirring. After that, the catalyst was isolated from the medium and added with 3.65 ml of glycerol. Further reaction proceeded for the next 3 h at the same reaction conditions. The conversion and yield percentage of glycerol and solketal were determined and correlated with the reaction without a catalyst, as shown in Figure 5.12. This study shows that the catalyst was not available in substantial amounts in the filtrate, which showed the heterogeneous nature of the modified catalyst. XRD analysis of the designed catalyst shows the same plots as that of a reused catalyst in Figure 5.13. Similarly, SEM analysis showed the same morphology as the recovered catalyst shows, confirming the stability of the repeated reuse catalyst Figure 5. 4 (d).

**Table 5.4. Recycling experiments using SCAT (3:2) catalyst for solketal synthesis**

| Catalytic run | Glycerol conversion (%) | Total acidic site (mmol/g) |
|---|---|---|
| **1.** | 99 | 2.34 |
| **2.** | 96 | 2.29 |
| **3.** | 92 | 2.27 |
| **4.** | 89 | 2.25 |
| **5.** | 86 | 2.19 |

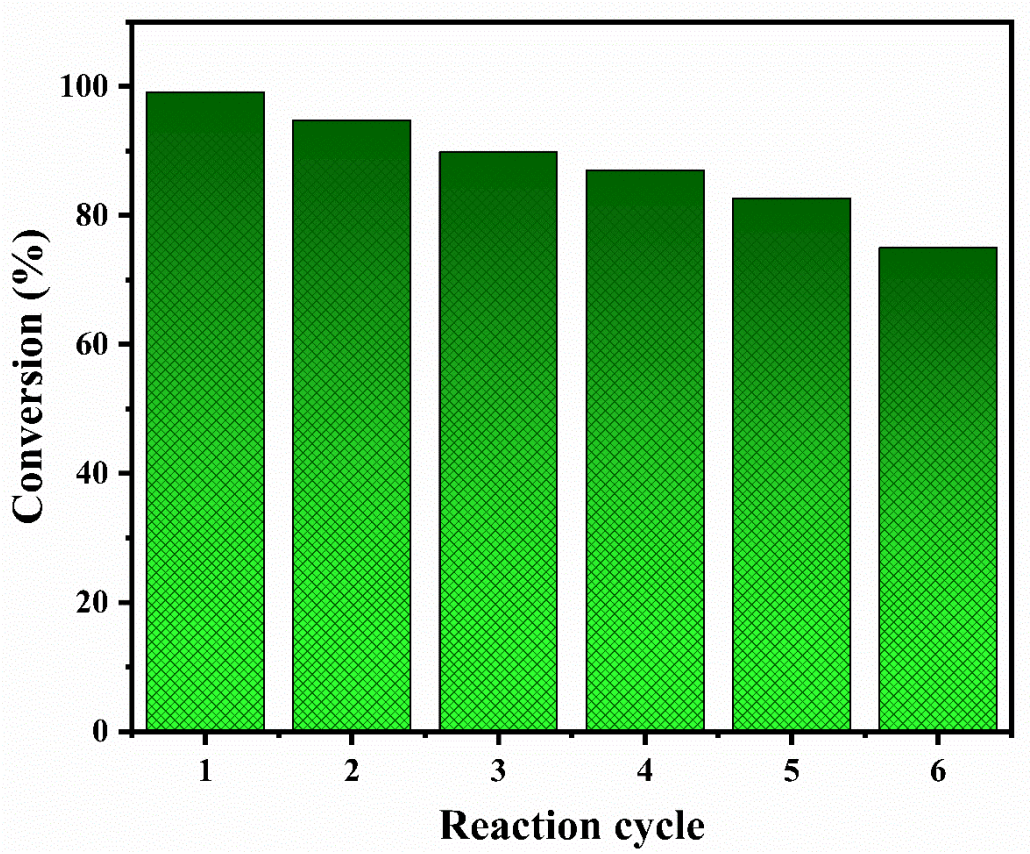


**Figure 5.11. Reusability test of synthesized SCAT catalys**

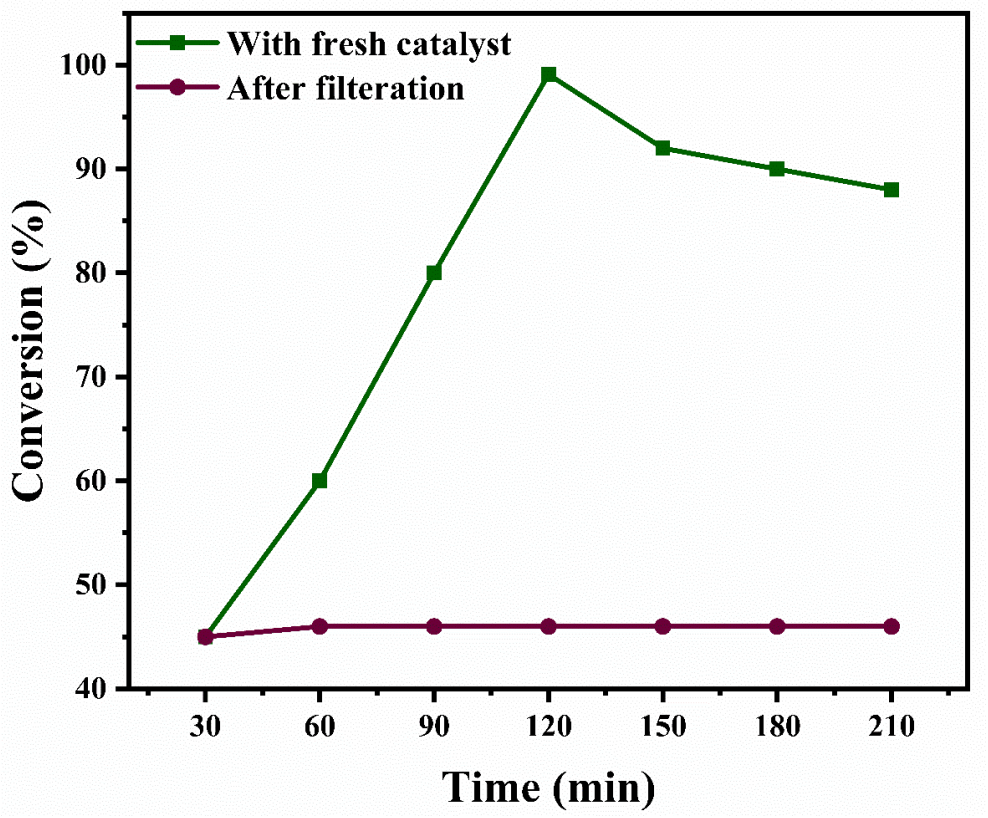


**Figure 5.12 Heterogenous nature of synthesized SCAT catalyst**

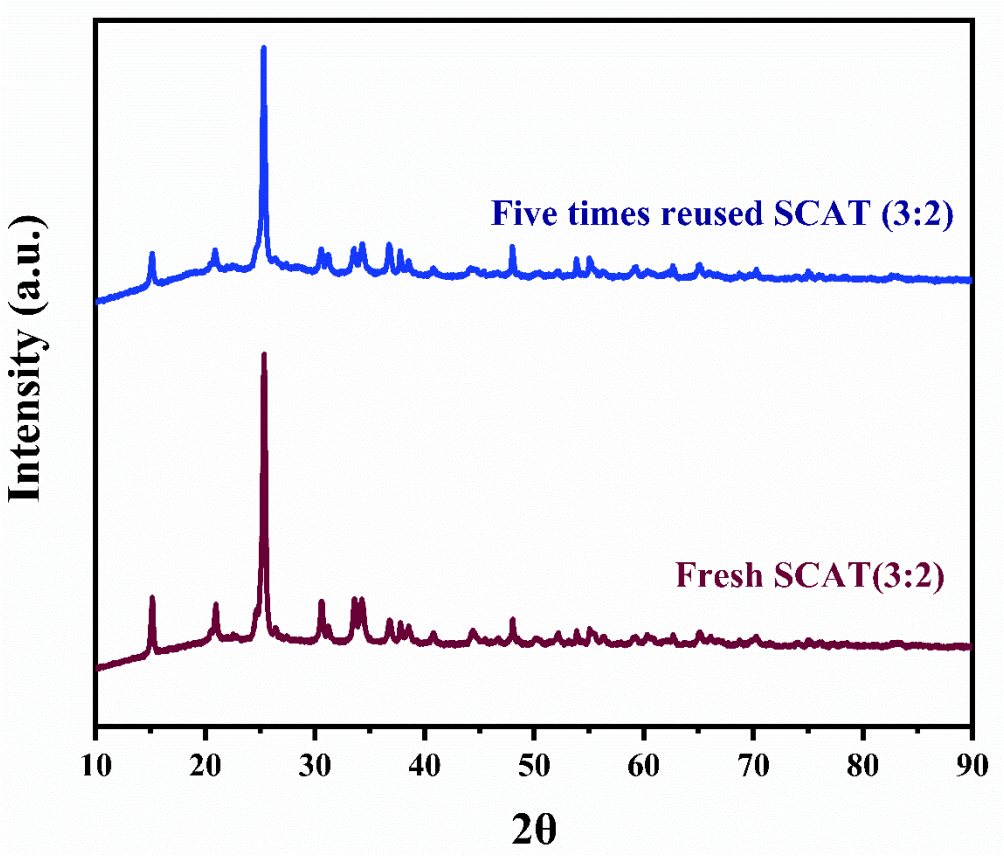


**Figure 5.13 XRD pattern of reused SCAT catalyst**

### 5.9 Comparative study

The catalytic efficiency, reusability, and stability of the designed SCAT catalyst with pioneer results towards solketal synthesis are compared with the other catalysts elaborated in Table 5.5. Catalysts like acid-activated clays [136] and Zeolites [137] showed high conversion of glycerol but needed a high duration of time. The catalytic activity of $Co[II](Co[III]_xAl_{2-x})O_4$ [138] and Al-SBA-15 [139] were very low and required high temperatures for glycerol conversion. Similarly, GS-$SO_3H$ catalyst [140] offered a good glycerol conversion and was highly recyclable up to the $5^{th}$ catalytic cycle, but the time duration was high. Other catalysts like $Fe(NO_3)_3.9H_2O$ [141] and $H_3PW_{12}O_{40}$ [142] required a high amount of acetone, but despite this, the conversion percentage was found to be very low. The catalyst's main drawbacks are the prolonged reaction time, high reaction temperature, low conversion, and vast amount of acetone needed. To tackle these

issues based on the aforementioned catalyst, author designed a heterogenous SCAT catalyst that displayed excellent catalytic activity and better solketal synthesis in a solvent-free medium. Therefore, the modified catalyst achieved 99 % glycerol conversion with 98 % solketal yield. In addition, the catalyst showed outstanding stability up to the fifth catalytic cycle at moderate reaction conditions compared to the reported catalysts.

**Table. 5.5. Comparison of synthesized SCAT (3:2) with previous reports**

| Catalyst | Reaction time (h) | Temp ($^{o}$C) | Molar ratio (Gly: Ace) | Glycerol Conversion (%) | Solvent | Endurance capacity | Ref. |
|---|---|---|---|---|---|---|---|
| $WO_3/SnO_2$ | 1.5 | RT | 1:1 | 55 | free | 5$^{th}$ reaction cycle | [69] |
| $MoO_3/SnO_2$ | 2.5 | RT | 1:1 | 71 | free | 5$^{th}$ reaction cycle | [69] |
| H-BEA | 1 | 60 | 1:4 | 72 | free | 5$^{th}$ reaction cycle | [70] |
| $SO_4^{-2}/SnO_2$ | 4 | RT | 1:1 | 95 | free | 5$^{th}$ reaction cycle | [71] |
| GS-$SO_3H$ | 4 | RT | 1:4 | 91 | free | 5$^{th}$ reaction cycle | [66] |
| Al-SBA-15 | 8 | 100 | 1:1(paraformaldehyde) | 75 | free | 5$^{th}$ reaction cycle | [65] |
| $H_3PW_{12}O_{40}$ | 2 | RT | 1:20 | 83 | free | 3$^{rd}$ reaction cycle | [68] |
| Algerian acid-activated clays | 48 | 40 | 1:4 | 89 | free | Not-reported | [62] |
| Zr-Mo-KIT-6 | 4 | 50 | 1:8 | 85 | free | 5$^{th}$ reaction cycle | [72] |
| $Fe(NO_3)_3.9H_2$ | 1 | 60 | 1:20 | 90 | free | 3$^{rd}$ reaction | [67] |

| | | | | | | | |
|---|---|---|---|---|---|---|---|
| O | | | | | | cycle | |
| Co[II](Co[III]$_x$ $Al_{2-x}$)$O_4$ | 3 | 130 | 1:10 | 69.2 | free | 5$^{th}$ reaction cycle | 64 |
| Zeolites (BEA, MFI, FAU) | 8 | 50 | 1:3 | 85 | Methanol | Not-reported | 63 |
| $MoO_3/SiO_2$ | 8 | 100 | 1:1(benzaldehyde) | 72 | Toluene | Not-reported | 27 |
| SCAT (3:2) (present work) | 2 | 58 | 1:10 | 99 | free | 6$^{th}$ reaction cycle | |

## 6. Conclusion

This study synthesized heterogeneous solid acid catalysts by the co-precipitation and wetness impregnation process. The cubic $CoAl_2O_4$ was synthesized by the co-precipitation process and followed by the wetness impregnation process to produce the active SCAT (3:2) acidic phase. The designed catalysts were found to be very efficient for the acetalization of bio-waste glycerol (a byproduct of biodiesel) with acetone. The acidic strength of the catalysts plays an important role in high conversion of glycerol and excellent solketal yield percentage. Various descriptive methods like XRD, FE-SEM, TGA, FTIR, BET surface area, N-butylamine titration, and XPS confirmed the existence of mixed oxide at different loading amounts and sulfur impregnation. $^1H$, $^{13}C$-NMR, and GC-MS were also used to analyze synthesized solketal quantitatively. Various reaction parameters were also optimized and achieved at optimized conditions to obtain the high glycerol conversion. The calculated value of TOF for the synthesized catalyst is 0.18 ($molg^{-1}h^{-1}$), which signifies good catalytic activity toward solketal synthesis. The catalyst was reusable up to 6$^{th}$ consecutive catalytic cycles, which reveals the high stability of the catalyst. The green chemistry metrics study showed that the solketal synthesis follows a greener route and is environmentally benign in nature. Overall, optimum reaction

conditions, short duration time, high selectivity, and catalyst recyclability proved to be more efficient, which can be suitable for sustainable solketal production on an industrial scale.